Guidelines for optimal selection of working fluid for an organic Rankine cycle in relation to waste heat recovery

Hærvig, Jakob; Sørensen, Kim; Condra, Thomas Joseph

Published in:
Energy

DOI (link to publication from Publisher):
10.1016/j.energy.2015.12.098

Publication date:
2016

Document Version
Accepted author manuscript, peer reviewed version

Citation for published version (APA):
Hærvig, J., Sørensen, K., & Condra, T. J. (2016). Guidelines for optimal selection of working fluid for an organic Rankine cycle in relation to waste heat recovery. *Energy*, *96*, 592-602.
https://doi.org/10.1016/j.energy.2015.12.098

Guidelines for Optimal Selection of Working Fluid for an Organic Rankine Cycle in Relation to Waste Heat Recovery

J. Hærvig[a,*], K. Sørensen[a], T.J. Condra[a]

[a] *Aalborg University, Department of Energy Technology, Pontoppidanstræde 111, DK-9220 Aalborg, Denmark*

Abstract

General guidelines on how to choose the optimal working fluid based on the hot source temperature available are reported. Based on a systematic approach, 26 commonly used working fluids are investigated by optimisations at hot source temperatures in the range 50-280 °C at intervals of 5 K. The genetic optimisation algorithm is used to optimise net power output by an optimal combination of turbine inlet pressure and temperature, condenser pressure, hot fluid outlet temperature, and mixture composition for mixtures.

The results suggest that the optimum working fluid in terms of maximum net power output has a critical temperature approximately 30-50 K above the hot source temperature. When two or more fluids with the same critical temperature are available, the ones with a positive slope of vapour saturation line are generally favoured. When mixtures are considered, the optimal mixture composition should be chosen so that the critical temperature of mixture is approximately 30-50 K below the hot source temperature and the temperature glide during condensing should approximate the temperature rise of the cold source.

Keywords: Working fluid selection, Organic Rankine cycle, Optimisation, Mixtures, General guidelines, Critical temperature

1. Introduction

To help reduce the consumption of fossil fuels, some currently non-utilised low-grade heat sources can be used. Heat sources with temperatures in the range 50-280 °C are found in numerous places ranging from geothermal sources to waste heat from process industries to marine vessels. For these purposes, the Rankine cycle can be implemented to convert thermal energy into mechanical or electrical power. Traditionally, water has been used as working fluid due to the fact that it is both chemically stable, non-toxic, non-flammable, environmental friendly, cheap, and widely available [1]. Organic fluid alternatives do however exhibit thermodynamic properties that make them highly suited for extracting energy at low temperatures. As pointed out by Tchanche et al. [1] these include a lower heat of vapourisation, lower temperature and pressure for the evaporation process, an expansion process that ends up in the vapour region, and a lower pressure ratio between evaporation and condensation resulting in a smaller turbine requirements. Other important thermodynamic properties include significantly lower critical temperatures and pressures, lower specific volume and different transport properties resulting generally in worse heat transfer characteristics and therefore different heat exchanger requirements. Furthermore, characteristics such as toxicity, flammability, fluid cost, ozone depletion potential, and global warming potential should be considered as well.

Due to the above mentioned differences, much research has already been carried out on ORC (organic Rankine cycles) for utilising low-grade energy with temperatures in the range 50-280 °C. Some studies mainly focus on cycle design or working parameters while others focus mainly on working fluid selection. Some limit their research to a particular application with a single hot source temperature while other study different cases having different hot source temperatures. The literature overview by Bao and Zhao [2] gives a great overview of the amount of literature dealing with working fluid selection. Furthermore, the study sums up the recommendations for working fluid selection for different hot source temperature ranges presented in the literature.

While some studies investigate and optimise the molecular composition of the working fluid by CAMD (computer aided molecular design) [3], other studies focus on more or less sophisticated equations of state to predict the properties of pure fluids and mixtures to model the cycles and compare the fluids in terms of first or second law efficiency, net power output, or total irreversibility. Saleh et al. [4] used the BACKONE equation of state to screen the thermodynamic properties of 31 pure component working fluids resulting in a set of general guidelines on cycle design depending on the type of fluid. These guidelines suggest that the highest amount of energy can be transferred

*Corresponding author: Tel.: +45 22 50 81 31
Email address: jah@et.aau.dk (J. Hærvig)

to super-critical fluid whereas the high temperature sub-critical fluid provides the worst heat transfer. In terms of thermodynamic efficiency, the highest values are obtained for high boiling substances with overhanging saturation domes operated at sub-critical conditions. Newer studies do however typically rely on the state-of-the-art commercially available REFPROP library by Lemmon et al. [5] to estimate thermodynamic and transport properties of both pure fluids and mixtures. This thermodynamic database relies on experimentally obtained equations of state.

Studies on zeotropic mixtures include Heberle et al. [6], Radulovic and Castaneda [7] who reports second law increments of up to 15 % by utilising mixtures instead of the pure fluids involved. Studies such as Li et al. [8], Andreasen et al. [9] point out how the temperature glide results in a better thermal match between the hot source and working fluid but results in larger heat exchanger areas as well. The study by Prasad et al. [10] does however suggest the required expander size to decrease when zeotropic mixtures are utilised.

The study by Maraver et al. [11] presents a systematic approach where cycles with R134a, R245fa, Solkatherm, m-Pentane, Octamethyltrisiloxane, and Toluene are optimised. Based on these optimisations, guidelines on how to maximise the exergy efficiency are given. One conclusion is that the heat capacity flow of the hot source should be similar to the heat capacity flow of the working fluid. Furthermore, the working fluids whose critical temperature is much lower than the hot source temperature result in lower thermodynamic performance. The results presented by Braimakis et al. [12] for hot source temperatures in the range between 150 and 300 °C suggest the optimal fluids in terms of exergy efficiency to be mixtures when the hot sources temperature exceeds 170 °C. Furthermore, the study concludes that at below 170 °C, pure fluids in trans-critical cycles perform better.

Common for most fluid selection studies in relation to organic Rankine cycles is that they typically consider a single or set of cases with a specific hot source temperatures. As pointed put by the literature review by Lecompte et al. [13], the difference in boundary conditions, makes a direct comparison between the studies a challenge. Therefore, a recent trend in ORC studies is to propose more general guidelines whenever possible. Xu and Yu [14] screened 57 fluid candidates to be used with a flue gas hot source. The study suggests that the optimal fluids candidates in terms of thermal efficiency have critical temperature in the range of 20-30 K below to 100 K above the hot source temperature. Other recent studies report optimal and constant values of $T_{\mathrm{crit}}/T_{\mathrm{hf,in}} \approx 0.5$ [9], $T_{\mathrm{crit}}/T_{\mathrm{hf,in}} \approx 0.8$ [15], which focus on two or three hot source temperatures respectively. The recent fluid selection study by Vivian et al. [16] investigated three different hot source temperatures of 120 °C, 150 °C, and 180 °C. Based on the results given in this study, the optimal fluids have $T_{\mathrm{crit}} - T_{\mathrm{hf,in}} \approx 35$ °C, which is quite different from the previous studies.

By varying the hot source temperature and investigating a high number of commonly used working fluids, the purpose of this study is to establish a set of guidelines which can be used as preliminary design tool when a Rankine cycle is to be designed for a specific purpose. These guidelines extend the ones by [16] and gives a secondary selection criterion that can be used, when more fluids have approximately the same critical temperature. First the applicability of the working fluid selection guideline presented by Vivian et al. [16] is extended to the temperature range 50°C to 280°C as this interval covers most low temperatures ranging from geothermal sources at 50°C to exhaust gas from marine engines at 280°C. Secondly, it is shown that the slope of vapour saturation line can be used to choose between two fluids having the approximately same critical temperature, both fulfilling the guideline presented by Vivian et al. [16]. Lastly, a set of mixtures are investigated to show that the already presented guidelines are shown to be applicable for mixtures as well.

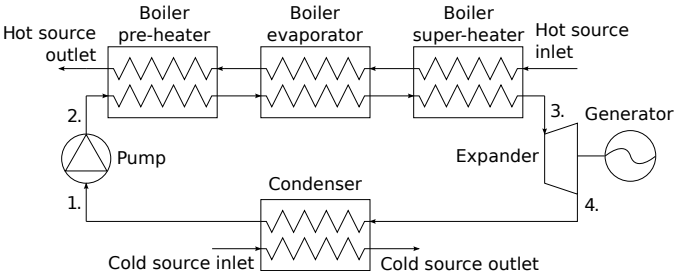

Figure 1: Schematic of the Rankine cycle considered along with annotations used in this study.

2. Modelling Approach

2.1. System and Parameter Overview

The basic Rankine cycle consisting of a pump, pre-heater, evaporator, super-heater, turbine, and a condenser illustrated in figure 1 is considered. The working fluid leaves the condenser as saturated liquid (point 1), is pumped to a higher pressure (point 2), is heated at constant pressure in the boiler to a given temperature to either saturated vapour or superheated vapour (point 3), is expanded in a turbine (point 4), and is condensed before entering the pump again (point 1). Depending on the fluid and hot source temperature considered, the cycles are either sub-critical or trans-critical depending on how the maximum net power output can be obtained.

The parameter of interest in this study is mainly the net work output defined by:

$$W_{\mathrm{net}} = \dot{m}_{\mathrm{wf}} \left(h_3 - h_4 - h_2 + h_1 \right), \tag{1}$$

This parameter describes how much power the given Rankine cycle is able to produce under the given conditions. Table 1 lists the conditions and parameters used in the study and if they are independent, dependent, or constant values throughout the analysis. The parameters are chosen to re-

Table 1: Modelling parameters in the analysis.

Parameter	Symbol	Value
Hot source		
Hot fluid		Dry air
Hot source inlet temperature	$T_{\mathrm{hf,in}}$	[50;280] °C
Hot source outlet temperature	$T_{\mathrm{hf,out}}$	indep.
Hot source pressure	P_{hf}	1.5 bar
Pinch point temperature in boiler	$T_{\mathrm{pp,boil}}$	10 K
Hot source mass flow rate	$\dot{m}_{\mathrm{hf}}$	150 kg/s
Cold source		
Cold fluid		Water
Cold source inlet temperature	$T_{\mathrm{cf,in}}$	15 °C
Cold source outlet temperature	$T_{\mathrm{cf,out}}$	20 °C
Cold source pressure	P_{cf}	1.5 bar
Pinch temperature in condenser	$T_{\mathrm{pp,cond}}$	5 K
Cold source mass flow rate	$\dot{m}_{\mathrm{cf}}$	depen.
Cycle parameters		
Turbine inlet temperature	$T_{\mathrm{turb,in}}$	indep.
Working fluid mass flow rate	$\dot{m}_{\mathrm{wf}}$	depen.
Boiling pressure	P_{boil}	indep.
Condensation pressure	P_{cond}	indep.
Working fluid composition	χ	indep.
Pump isentropic efficiency	η_{pump}	0.8
Turbine isentropic efficiency	η_{turb}	0.8
Number of boil. discretisations	n_{boil}	40
Number of cond. discretisations	n_{cond}	40

semble the conditions in waste heat recovery systems. To be able to compare the results to other systems using different hot sources than dry flue gas, the heat capacity rate $\dot{c_{\mathrm{p}}} = \dot{m} \cdot c_{\mathrm{p}}$ is used as a unique parameter. This parameter defines the rate at which temperature changes as energy is transferred. Estimating $\dot{c_{\mathrm{p}}}$ based on the hot source mass flow of 150 kg/s, the heat capacity rate is almost constant at values between 151 kJ/(K·s) and 156 kJ/(K·s) for inlet temperatures in the range between 50 °C and 280 °C.

As shown in table 1, a constant mass flow rate of 150 kg/s is used in this study. It is however important to note that it does not affect the guidelines presented in this study. That is, a unit mass flow rate could have been used as well, resulting in the exact same guidelines. The mass flow rates of the working fluid and cold source and the net power output are simply scaled accordingly.

2.2. Heat Transfer Modelling

The energy transferred in the heat exchangers can be estimated by the overall heat transfer coefficient U, the heat transfer area A, and the mean temperature difference at which energy is transferred:

$$\dot{Q} = UA\Delta T_{\mathrm{lm}}, \tag{2}$$

where details on how the temperature difference is evaluated are given in subsection 2.3. Instead of applying partly validated correlations for U to cover all the different fluids, conditions, and mixtures considered in this study, UA values are reported. The UA value for a heat exchanger is a measure of the required heat exchanger size. For this study, where the hot source is flue gas with a low Prandtl number, the heat transfer in the boiler is limited by the flue gas side heat transfer as stated by Roetzel and Spang [17]. When mixtures are considered, the boiling and condensing heat transfer coefficients differ significantly as described by Cheng and Mewes [18]. For this study transient effects due to fouling and start-up of the system are not considered. As UA values are reported, the reader can use their own heat exchangers with known UA values to get the results reported.

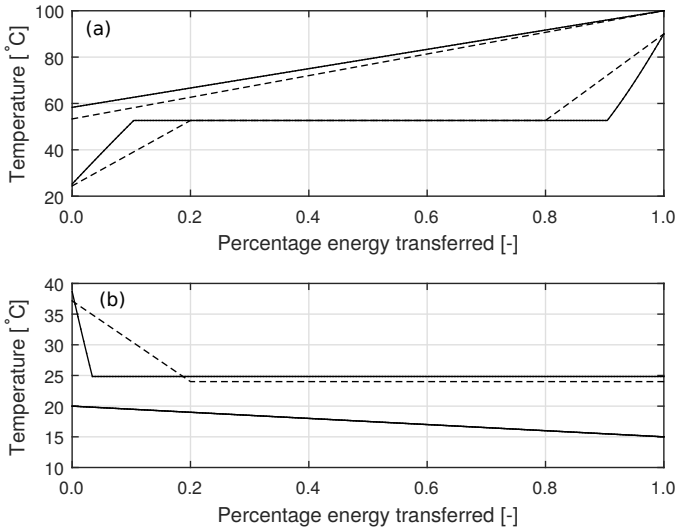

Figure 2: Comparison of T-Q profiles for ammonia being heated by a hot source at 100°C with different number of discretisations n in: (a) Boiler with $n = 5$, - - -, $n = 10,000$, ——; (b) Condenser with $n = 5$, - - -, $n = 10,000$, ——.

2.3. Heat Exchanger Discretisation

As already pointed out by Maraver et al. [11], the heat exchanger discretisation is important to resolve the heat transfer process. For this study, where fixed pinch points in the boiler and condenser are used, the pinch point location is unknown before modelling the process. Furthermore, as the additional computational time is proportional to the number of discretisations, it is a important in order to keep the overall computational time of the optimisations as low as possible low. Therefore, a discretisation analysis is carried out in the present study to find a reasonable number of discretisation for a typical heat exchanger process. The trans-critical process having almost parallel T-Q profiles for the hot source and working fluid does not require a high number of discretisations to resolve the process. Therefore, focus is on the sub-critical boiling and condensation processes. Figure 2(a) and (b) show examples of a sub-critical boiling process and condensation process using ammonia as the working fluid being heated by hot source at 100 °C. The pressure levels and turbine inlet temperature, and hot source outlet temperature are found by the optimisation process presented in this study.

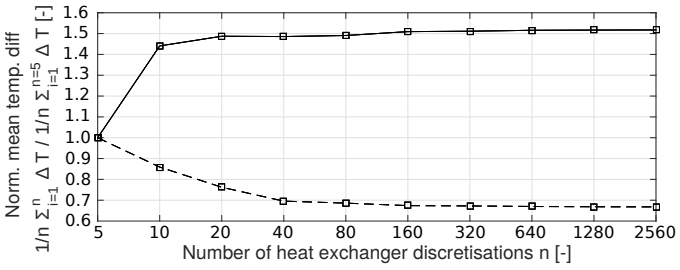

Figure 3: The influence of number of discretisations on the mean temperature difference between hot/cold source and the working fluid being ammonia and hot source at 100 °C in this example: Boiler, ——, condenser, - - -.

Each process is discretised with $n = 5$ and $n = 10,000$ to illustrate the difference between a coarse and very fine discretisation.

As the figure shows, the discretisation used influences the amount of energy extracted from the hot source. To quantify the effect of discretisation, figure 3 shows the mean temperature difference with different number of discretisations in the range [5;2560] normalised by the mean temperature difference with 5 discretisations.

Based on the results in figure 3, the heat exchangers are discretised into 40 sections. These discretisations are both used when evaluating the pinch point location using T-Q profiles and when calculating the mean temperature difference ΔT_{lm} by:

$$\Delta T_{\mathrm{lm}} = \frac{1}{n}\sum_{i=1}^{n}\Delta T_i \tag{3}$$

2.4. Working Fluids and Their Thermodynamic Properties

A list containing the 26 fluids candidates considered in this study is given in table 2. These fluids investigated are fluids commonly reported in literature.

Along with the critical temperature and pressure, the inverse of the slope of vapour saturation line $\xi = \mathrm{d}s/\mathrm{d}T$ on the T-s diagram is given. This parameter, first proposed by Liu et al. [37] has been suggested in other studies along with the critical point to be key parameters when determining the maximum potential of a given fluid at a given hot source temperature. In this study, ξ is evaluated at $\mathrm{d}s^2/\mathrm{d}T^2 = 0$ for dry fluids and at 20°C for wet fluids corresponding to approximately the condensing temperature. If $\mathrm{d}s^2/\mathrm{d}T^2 = 0$ does not exist between 20°C and T_{crit}, then it is evaluated at 20°C for dry fluids as well. This approach has been used for all the fluid candidates investigated in this study and is found to give representative values of xi for the cycles considered. Examples are given in figure 4 with pentane and propane as dry and wet fluids respectively. The figure shows both the pure fluids and how the saturation dome is altered by different mixture compositions.

As research still goes on to improve the equation of states for the different fluids, the references for the equations of states used in this study are given in the last column in table 2.

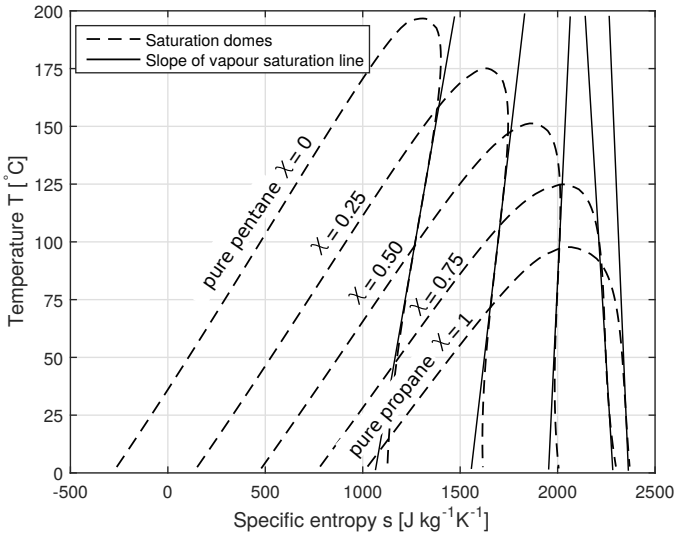

Figure 4: Saturation domes for a propane-pentane mixture of compositions 0/1 (pure pentane), 0.25/0.75, 0.50/0.50, 0.75/0.25, and 1/0 (pure propane). The slope of vapour saturation lines ξ evaluated at the evaluation criterion used in this study are shown as well. Note that the lines shown correspond to $\xi^{-1} = \mathrm{d}T/\mathrm{d}s$.

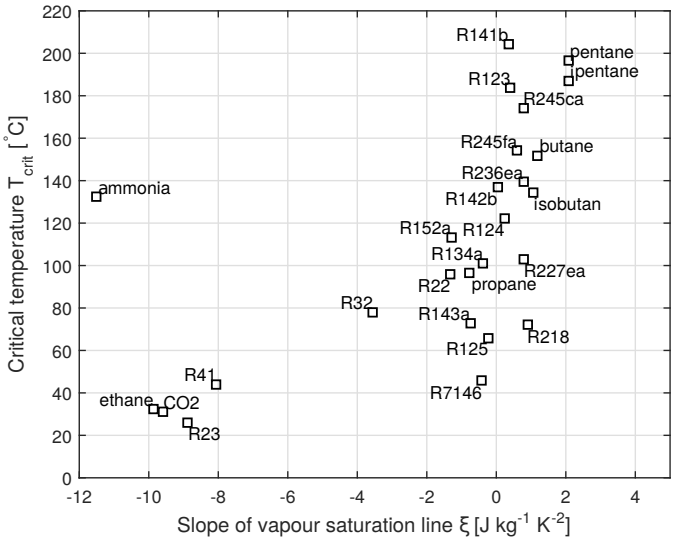

Figure 5: Critical temperature as function of slope of vapour saturation line for the pure fluid candidates considered in this study.

To visualise the slope of vapour saturation line and critical temperatures of the fluids considered, figure 5 is used. To evaluate thermodynamic properties for the fluids the extensive REFPROP library by Lemmon et al. [5] is used, as reviews of thermodynamic databases such as Ziviani et al. [38] suggests the REFPROP library to be the most complete in terms of available fluids and accuracy. Typical accuracies are 0.1% in densities, 1% in heat capacities, 1% in speed of sound, and 0.2% in vapour pressure. The uncertainties do however vary by small amounts for the different fluids and for some fluids the exact uncer-

Table 2: Working fluids considered in this study along with their critical point, inverse slope of vapour saturation line, and chemical name and listed by their ASHRAE number.

Number	Chemical name	T_{crit} [°C]	P_{crit} [bar]	ξ [J/(kg K^2)]	Equation of state
R22	chlorodifluoromethane	96.2	5.0	-1.32	Kamei et al. [19]
R23	trifluoromethane	26.1	4.8	-8.87	Penoncello et al. [20]
R32	difluoromethane	78.1	57.8	-3.55	Tillner-Roth and Yokozeki [21]
R41	fluoromethane	44.1	59.0	-8.05	Lemmon and Span [22]
R123	2,2-dichloro-1,1,1-trifluoroethane	183.7	36.6	0.41	Younglove and McLinden [23]
R124	2-chloro-1,1,1,2-tetrafluoroethane	122.3	36.2	0.24	de Vries et al. [24]
R125	pentafluoroethane	66.0	36.2	-0.23	Lemmon and Jacobsen [25]
R134a	1,1,1,2-tetrafluoroethane	101.1	40.6	-0.37	Tillner-Roth and Baehr [26]
R141b	1,1-dichloro-1-fluoroethane	204.4	42.1	0.35	Lemmon and Span [22]
R142b	1-chloro-1,1-difluoroethane	137.1	40.6	0.03	Lemmon and Span [22]
R143a	1,1,1-trifluoroethane	72.7	37.6	-0.75	Lemmon and Jacobsen [27]
R152a	1,1-difluoroethane	113.3	45.2	-1.29	Outcalt and McLinden [28]
R170	ethane	32.2	48.7	-9.86	Buecker and Wagner [29]
R218	octafluoropropane	71.9	26.4	0.89	Lemmon and Span [22]
R227ea	1,1,1,2,3,3,3-heptafluoropropan	101.8	30.0	0.79	Lemmon and Span [22]
R236ea	1,1,1,2,3,3-hexafluoropropane	139.3	35.0	0.78	Huber and Ely [30]
R245ca	1,1,2,2,3-pentafluoropropane	174.4	39.3	0.77	Huber and Ely [30]
R245fa	1,1,1,3,3-pentafluoropropane	154.0	36.5	0.61	Lemmon and Span [22]
R290	propane	96.7	42.5	-0.76	Lemmon et al. [31]
R600	butane	152.0	38.0	1.19	Buecker and Wagner [32]
R600a	isobutane	134.7	36.3	1.07	Buecker and Wagner [32]
R601	pentane	196.6	33.7	2.07	Jaeschke and Schley [33]
R601a	ipentane	187.2	33.8	2.09	Lemmon and Span [22]
R717	ammonia	132.3	113.3	-11.52	Tillner-Roth and Baehr [34]
R744	carbon dioxide	31.0	73.8	-9.58	Span and Wagner [35]
R7146	sulfur Hexaflouride (SF6)	45.6	37.6	-0.41	Guder and Wagner [36]

tainty remains undocumented. Transport properties are not modelled as neither the heat exchangers nor the pressure loss is modelled.

To model exact T-s profiles, temperature dependent heat capacities are taken into account for both sources. The hot source is modelled as a combination of 21% oxygen, 78% nitrogen, and 1% argon on mole basis, which corresponds to atmospheric air, as atmospheric air and flue gas contains almost the same thermodynamic properties (within 2-3 %). The cold source is modelled as pure water according to the equation of state presented by Wagner and Pruss [39] and implemented in the REFPROP library.

3. Optimisation

3.1. Definition of Optimisation Problems

The optimisation problem considered will be to maximise the net work output by optimal combination of turbine inlet temperature and pressure, hot source outlet temperature, and condensing pressure. For mixtures, the mixture composition χ is optimised as well. A set of constraints is set up to allow only thermodynamically feasible designs that do not violate the specific minimum pinch point temperatures given in table 1. As the optimisation is carried out for different fluid candidates and different hot source temperatures, the constraints vary for every optimisation. For example the minimum condenser pressure depends on the saturation pressure, which is fluid dependent. The following expresses the optimisation in a general manner:

$$\begin{aligned}
\text{maximise:}\quad & W_{\text{net}} = f\left(T_{\text{turb,in}}, P_{\text{turb,in}}, T_{\text{hf,out}}, P_{\text{cond}}, \chi\right), \\
\text{subject to:}\quad & T_{\text{cf,in}} + T_{\text{pp,cond}} \leq T_{\text{turb,in}} \leq T_{\text{hf,in}} - T_{\text{pp,boil}}, \\
& T_{\text{cf,in}} + T_{\text{pp,cond}} + T_{\text{pp,boil}} \leq T_{\text{hf,out}} \leq T_{\text{hf,in}}, \\
& P_{\text{sat@}T=T_{\text{cf,in}}} \leq P_{\text{cond}} \leq P_{\text{turb,in}}, \\
& P_{\text{cond}} \leq P_{\text{turb,in}} \leq 200 \text{ bar}, \\
& 0 \leq \chi \leq 1, \\
& 1 \leq x_{\text{turb,out}},
\end{aligned} \tag{4}$$

where χ denotes the mass fraction of the first-mentioned substance for a given mixture and $x_{\text{turb,out}}$ is the quality of the fluid at the outlet of the turbine. This optimisation process described by (4) is carried out of every fluid in table 2 at hot source temperatures ranging from 50 to 280°C at intervals of 5 K.

3.2. Considerations on Convergence

For the optimisations carried out in this study, the MATLAB implementation of the genetic algorithm first

Table 3: Settings for the genetic algorithm used for optimisation.

Parameter	Value
Maximum number of generations	300
Maximum number of stalled generations	50
Maximum tolerance within stalled generations	10^{-10}
Population size	50
Crossover fraction	0.8
Elite count	2

presented by Holland [40] is used. By using the genetic algorithm, the global optimum is found by a successive series of cross-over and mutation operations. For this study, convergence is assumed when the average relative change in net power output is 10^{-10} over 50 stalled generations. This criterion is chosen to ensure the true optimum is found. Table 3 gives an overview of the settings used for genetic algorithm.

Running the same optimisation multiple times with the settings in table 3 is found to give consistent results. This suggests that the optimisation algorithm has successfully found the true optimum.

3.3. Validation of Results Obtained

To make sure that the results obtained by the thermodynamic models are accurate, and that the optimisation process convergences to the optimum with reasonable accuracy, the results are compared to results reported in literature. To ensure sufficient convergence is obtained for both optimisation algorithms, the modelling parameters in table 1 are changed to fit those in other studies and the results are compared. Andreasen et al. [9] presents results for $T_{\mathrm{hf,in}} = 120$ °C and $T_{\mathrm{hf,in}} = 90$ °C for the simple ORC for both pure fluids and mixtures. The results obtained by the model in this study deviate less than 3% when comparing quantities such as boiler and condenser pressure, and turbine inlet temperature. Other studies used for comparison include Walraven et al. [41], Dai et al. [42], and Chys et al. [43].

3.4. Visualisation of Parameters and Objective Function

As multiple parameters are considered in this optimisation, a way to visualise the results of the optimisations is required. Figure 6 visualises the results of the optimisation by relating the different parameters and the objective at a hot source temperature of 200 °C. For most fluid candidates, the almost parallel lines between the hot source outlet temperature, turbine inlet temperature, boiling pressure, and condensation pressure suggests these to be directly related. Four fluid candidates, namely R141b, R123, R245ca, and ammonia, the relation between hot source outlet temperature and turbine inlet temperature differs significantly. Inspection of the cycles for R141b, R123, and R245ca shows that these are all operated subcritically with a distinct evaporation process. The more

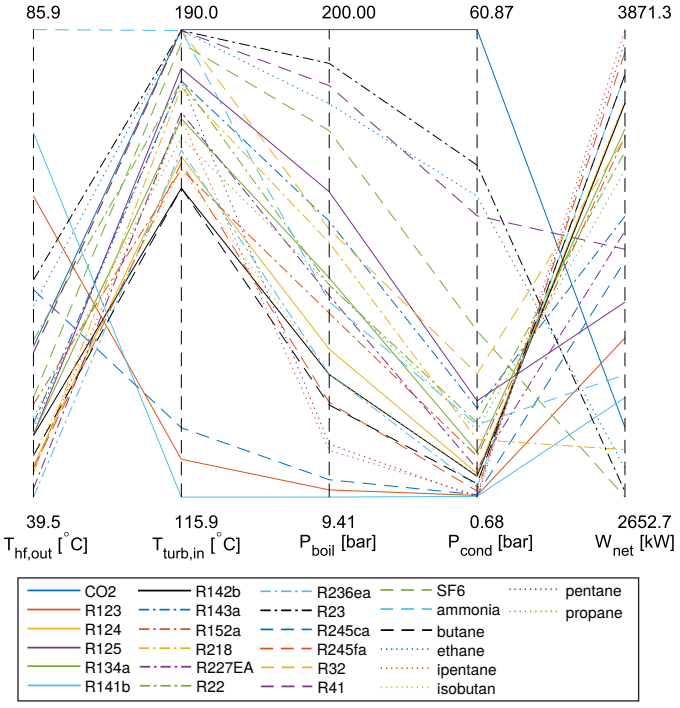

Figure 6: Paralle coordinates showing the how the parameters are linked to the objective function for the optimised cycles using the different fluid candidates at a hot source temperature of 200 °C.

dry fluids fluids having high critical temperatures like pentane and ipentane are expanded directly through the saturation dome after pre-heating resulting in the tri-lateral cycle, which is discussed in details in details in Fischer [44] and Ajimotokan and Sher [45].

4. General Considerations on Optimal Fluids Based on Optimisation

4.1. Pure Fluid Candidates

Figure 7 shows the maximum potential in terms of net power output W_{net} for some of the pure working fluid candidates at a varying hot source temperature $T_{\mathrm{hf,in}}$ in the range [50;280] °C with 5 K intervals. That is, each point in the figure corresponds to an optimal solution found by the genetic algorithm.

The results in the figure 7 shows how the maximum net power output in general increases with higher hot source temperatures. The maximum net power output that can be obtained for a given fluid increases exponentially at low hot source temperatures. At a certain transition point, the net power output begins to increase linearly with increasing hot source temperature. This critical point is observed to be fluid dependent and is found to occur when the optimal cycle changes from being sub-critical to trans-critical. When comparing the different fluids, the figure suggests that each fluid only has a single and limited range in which it is optimal. That is, a fluid resulting in high net power output at low temperatures will not perform as good at

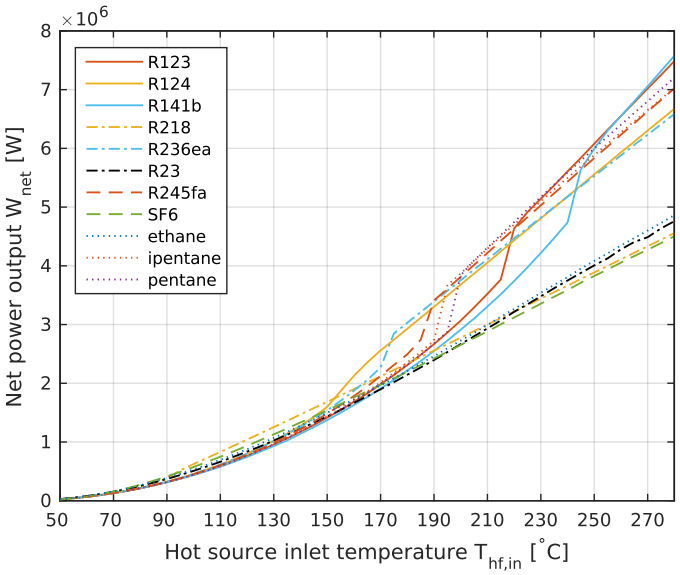

Figure 7: Optimal designs in terms otransferedf net power output for different working fluid at a varying hot source temperature in the range [50;280] °C.

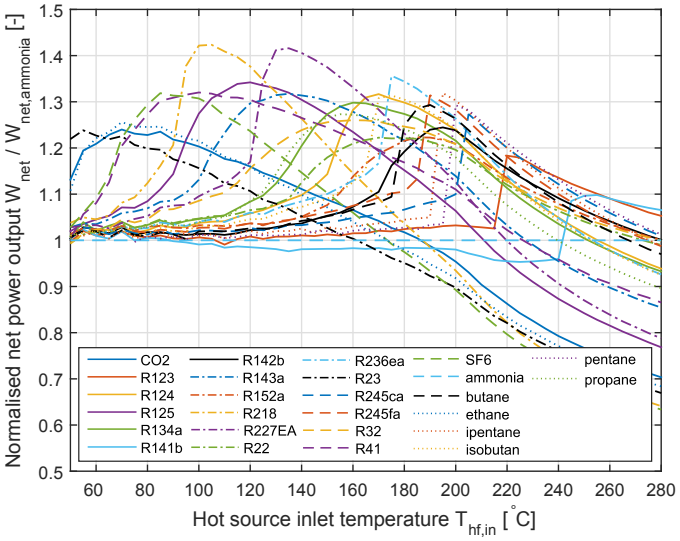

Figure 8: Optimal designs visualised by the net power output normalised by ammonia for different working fluids at a varying hot source temperature in the range [50;280] °C.

high temperatures when compared to other fluids. To better compare the results in figure 7, the optimised net power output is normalised by the optimised net power output for ammonia at the same hot source temperature. The normalised results are shown in figure 8. Using this approach, the different fluids have a certain hot source temperature at which the ratio $W_{\text{net}}/W_{\text{net,ammonia}}$ is maximum. Ammonia is chosen for comparison because it is a commonly used fluid in various cycles.

The figure shows how ammonia is outperformed or outperforms the different fluid candidates in terms of net power output at different hot source temperatures in the range [50;280] °C. If another fluid was used for comparison, this figure would look different, but the relative difference between the working fluid candidates would still be same. To investigate whether there is a correlation between the optimal fluid in the different hot source temperature intervals and their critical temperature, table 4 is used. This table lists the optimal working fluid candidates in terms of net power output in different hot source temperature ranges along with their critical temperature.

Table 4: The optimal working fluids in terms of net power output in different hot source temperature ranges.

Hot source temp. range [°C]	Fluid candidate	Critical temperature [°C]
[50;60]	R23	26.1
[65;70]	ethane	32.2
[75;90]	R7146	45.6
[95;120]	R218	71.9
[125;160]	R227ea	101.8
[165;170]	R124	122.3
[175;185]	R236ea	139.3
[190;190]	R245fa	154.0
[195;200]	ipentane	187.2
[205;235]	pentane	196.6
[240;255]	R123	183.7
[260;280]	R141b	204.4

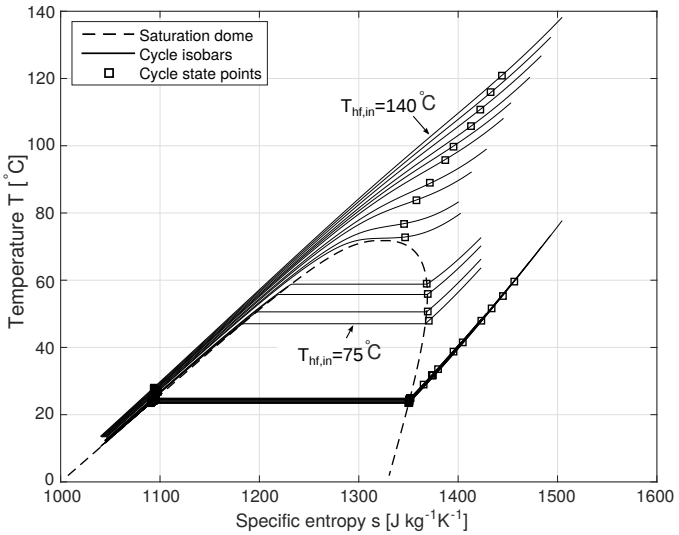

Figure 9: Optimal cycles for R218 with hot source temperatures in the range [75;140] °C with intervals of 5 K.

Table 4 shows how the best fluid candidates all should be operated at hot source temperatures above their critical temperature, which can be explained by a better thermal match with hot source temperature allowing for a better hot source utilisation. As an example, figure 9 shows the optimal cycles for R218 when the hot source temperature is varied between 75 °C and 140 °C. The figure shows that when the $T_{\text{hf,in}} = 95$ °C (approximately 25 K above the critical point) the optimal cycle is trans-critical resulting in a significantly better thermal match between the hot

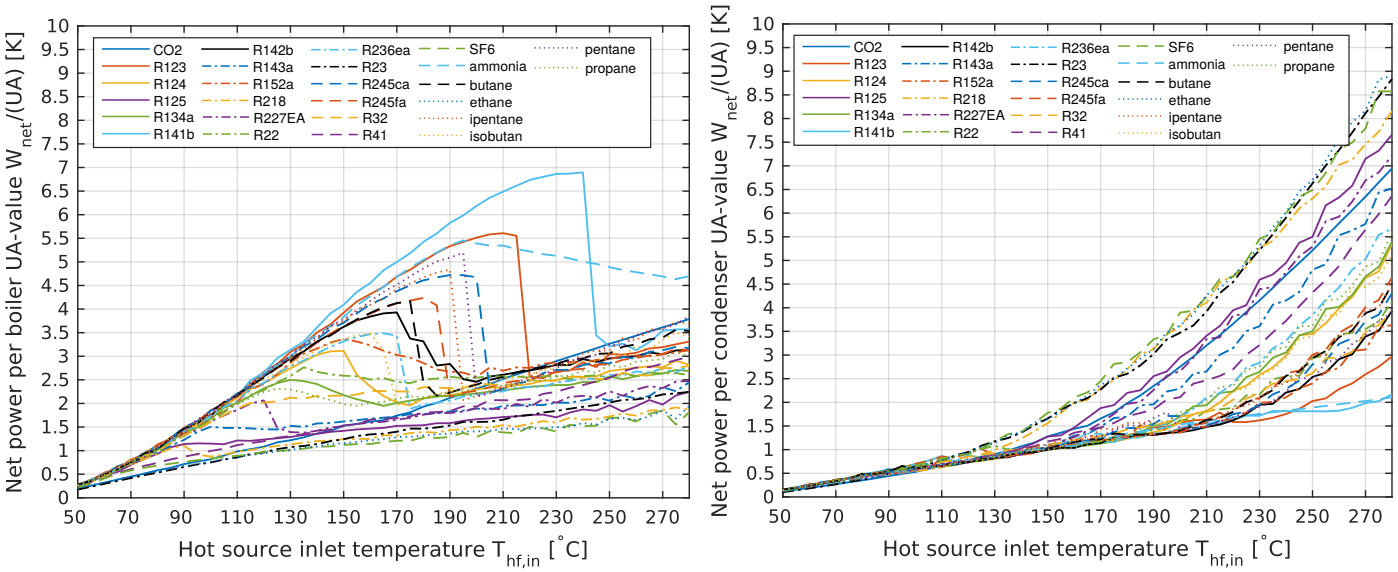

Figure 10: Optimal designs by net work output shown with net power output per heat exchanger UA-value for the condenser and boiler at a varying hot source temperature in the range [50;280] °C.

source temperature and working fluid. The result is a high net work output and consequently a low mean temperature difference. As heat is transferred at a lower mean temperature difference, the required heat exchanger size will be significantly higher. Figure 10 shows the net power output to heat exchanger UA-value for the boiler in 10(a) and condenser in 10(b) for the designs in figure 7. The results in figure 10(a) suggest the net power to boiler heat exchanger UA-value to increase with hot source temperature, until a certain hot source temperature where the ratio drops drastically. This sudden drop in net power to heat exchanger UA-value ratio can be explained by the optimal cycles going from sub-critical to trans-critical. Furthermore, the results suggest this sudden drop to be more evident for dry fluids having $\xi < 0$. On the other hand, fluids having $\xi \ll 0$ such as ammonia, ethane, CO_2, R23, and R41 do not show this behaviour. The results in figure 10(b) suggest the net power to condenser heat exchanger UA-value to increase throughout the hot source temperature range. This can be explained by the increasing net power output and the condenser UA-value being almost constant due to fixed conditions for the cold source.

The results in table 4 suggest that an optimal pure working fluid should have a critical temperature 30-50 K below the hot source temperature. As figure 8 suggested, all the working fluids have a temperature range in which they are significantly better than ammonia. For fluids having low critical temperatures such as R23, CO2, and Ethane, they outperform ammonia at low hot source temperatures. Likewise do the fluids having high critical temperatures such as R141b, pentane, ipentane, and R123 outperform ammonia and high hot source temperatures. This statement is in fact valid for all the working fluid candidates investigated in this study. Figure 11 shows the normalised net power output as function of temperature difference

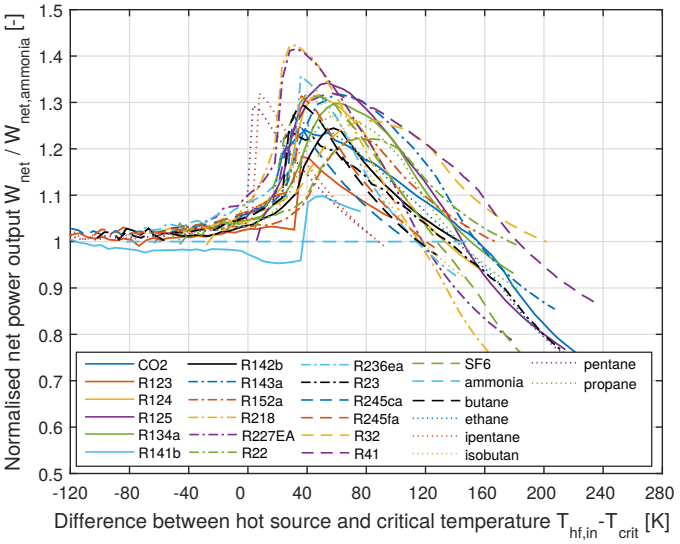

Figure 11: Normalised net power output as function of temperature difference between the hot source and critical temperature of the fluid candidates.

between the hot source inlet temperature and the critical temperature. As the figure suggests, all the candidates outperform ammonia when operated at a hot source temperature approximately 30-50 K above their critical temperature, that is $T_{\mathrm{hf,in}} - T_{\mathrm{crit}} = [30; 50]$ K. For fluids having $\xi \gg 0$ such as pentane and ipentane, $T_{\mathrm{hf,in}} - T_{\mathrm{crit}}$ should be slightly lower around $T_{\mathrm{hf,in}} - T_{\mathrm{crit}} = [0; 15]$ K but still operated at $T_{\mathrm{hf,in}} > T_{\mathrm{crit}}$. The results of this study therefore suggests that there is not a single $T_{\mathrm{hf,in}}/T_{\mathrm{crit}}$ parameter resulting in optimal performance. Instead, a optimal difference $(T_{\mathrm{hf,in}} - T_{\mathrm{crit}})$ exists, such that the performance is optimal for a given hot source temperature.

Two fluids candidates can however have the almost same

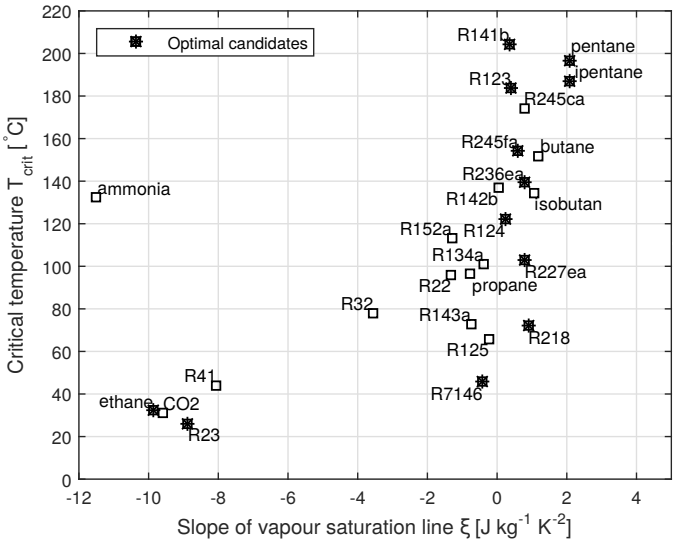

Figure 12: Optimal working fluid candidates shown in a critical temperature as function of slope of vapour saturation line chart.

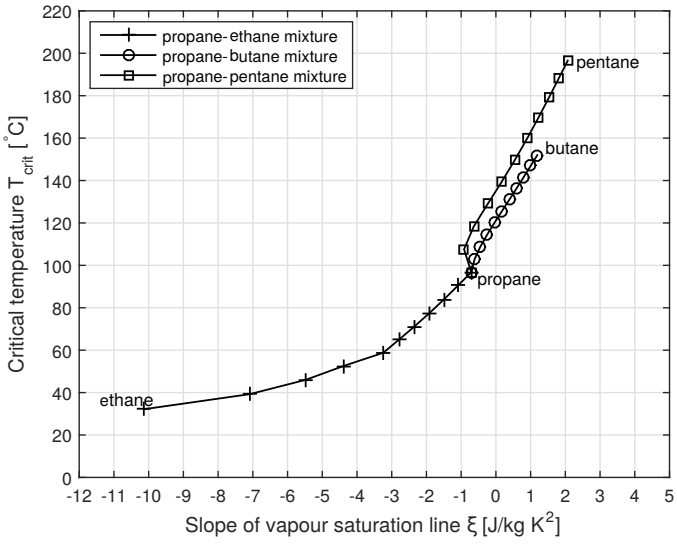

Figure 13: Critical temperature as function of slope of vapour saturation line for the mixtures considered in this study. Marks are placed at changes in mixture composition of 0.1.

critical temperature. Therefore, a criteria is set up to choose between two fluids having the approximately same critical temperature in order to obtain the maximum net work output. Studies from literature have suggested the the slope of vapour saturation line to play a major role as super heating can be avoided for fluids with $\xi > 0$. Figure 12 shows the optimal fluids from table 4 listed by their critical temperature and slope of vapour saturation line. Ethane and R23 being the optimal fluids for hot source temperatures in the range [50;70] have both $\xi \ll 0$. An alternative could have been R7146 (SF6) which only has a slightly higher critical temperature but $\xi \approx 0$. This result suggests the critical temperature to be more important than the slope of vapour saturation line, when looking for a working fluid for a given hot source temperature to obtain the maximum net power output. If fluids having critical temperatures similar to R23 and Ethane and slope of vapour saturation line close to zero were included, these are expected to perform better than R23 and Ethane. At hot source temperatures in the range [95;190], fluids having $\xi > 0$ are favoured when more fluid candidates have almost the same critical temperature, an example being R218 and R143a where R218 has $\xi > 0$ and R143a has $\xi < 0$. For mixtures, the critical temperature and slope of vapour saturation line depends on the mixture composition. In the following, considerations on the optimal mixture are given.

4.2. Mixture Candidates

By considering mixtures with the mixture composition as a design variable, the mixture composition χ can be used to alter the two parameters discussed until now. That is the critical temperature T_{crit} and slope of vapour saturation line ξ. How the position in the $T_{\text{crit}} - \xi$ chart is altered when the composition is shifted by 0.1 for the mixtures is shown in figure 13. Furthermore, the mixtures do as well introduce a temperature glide, which allows for a better thermal match with the hot and cold sources. This is especially important for the iso-thermal condensation and sub-critical boiling processes, which would otherwise introduce large irreversibilities. Figure 14 shows the temperature glide for the three mixtures as function of mixture composition for condensation processes where the mixtures leave the condenser at saturated liquid at 20 °C.

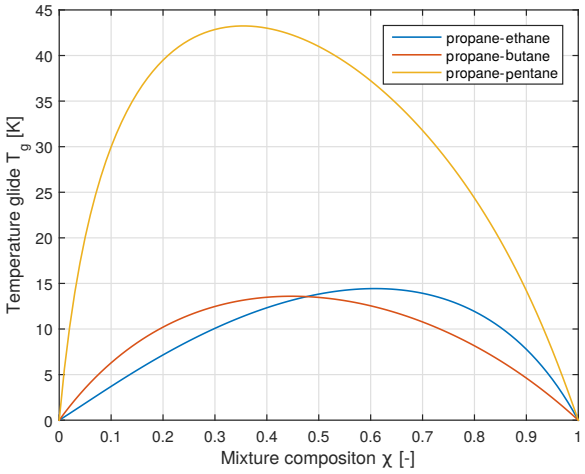

Figure 14: Temperature glide of the mixtures during condensation as function of the mixture composition when mixture leaves the condenser at saturated liquid at 20 °C.

Performing the optimisations for the mixtures with the mixture composition as an additional design variable, the results in figure 15 are obtained with the mixture compositions shown in figure 16.

As the mixture composition is found by optimisation, the mixtures should at least perform as good as the pure

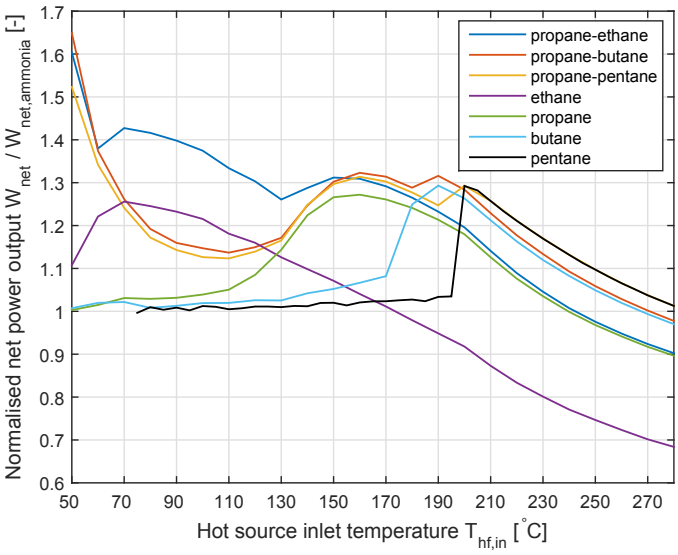

Figure 15: Optimal designs visualised by the net power output normalised by ammonia for different working fluid mixtures at a varying hot source temperature in the range [50;280] °C with intervals of 10 K. The pure fluid candidates from figure 8 are shown for reference.

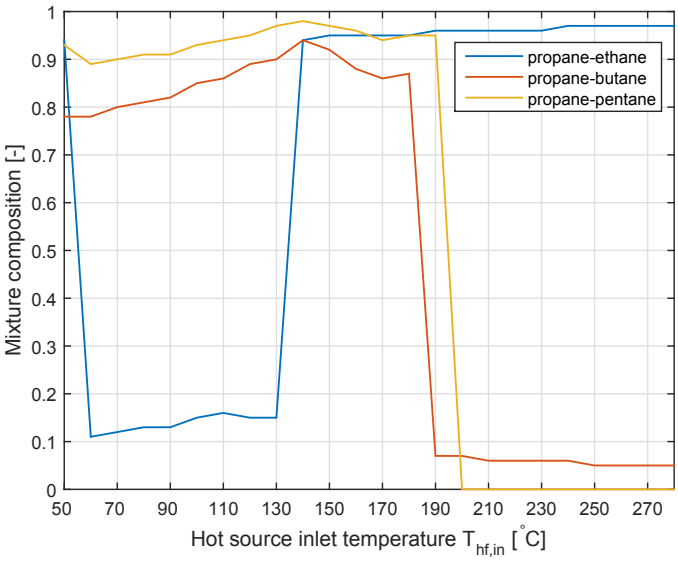

Figure 16: Optimal mixture composition at varying hot source temperatures in the range [50;280]°C with intervals of 10 K.

fluids used in the mixture. Figure 15 shows that this is actually the case. Furthermore, the figure shows that the mixtures in most cases perform better than the pure fluids with the exception of the propane-pentane mixture, which at hot source temperature above 200 °C perform similar to pure pentane. Figure 16 shows that the optimal mixture composition for the propane-pentane mixture is indeed 0 (corresponding to pure pentane) for $T_{\mathrm{hf,in}} > 200$ °C. That is, even though the condensation process can be improved by a better thermal match by adding propane to pentane, the lower critical temperature introduced by adding Propane results in lower net power output.

For the propane-butane mixture, the net power output is increased at all hot source temperatures, suggesting a temperature glide to increase the net power output even though the critical temperature is decreased slightly by the addition of propane. At lower hot source temperatures ($T_{\mathrm{th,in}} < 190$ °C), the optimal mixtures contain Propane fractions in the order of 0.8-0.9. At higher hot source temperatures ($T_{\mathrm{th,in}} > 190$ °C) the optimal mixture composition changes radically to consist of mostly butane. In all the hot source temperature interval, the mixture composition results in a temperature glide of approximately 5 K resulting in a good thermal match with the cold source.

For the propane-ethane mixture, the net power output is again increased in all the hot source temperature interval compared to the pure propane and ethane. Again a radical change in mixture composition is observed. For the propane-ethane mixture this transition occurs at 140 °C, where the optimal mixture composition changes from approximately 0.15/0.85 to 0.95/0.05. Both these mixture compositions result in a temperature glide of 5 K as seen in figure 14. As opposed to the other two mixtures, the propane-ethane mixture favours propane at higher temperatures ($T_{\mathrm{hf,in}} > 140$ °C). This can be explained by the fact that propane has a higher critical temperature than ethane.

To sum up, all three mixtures show that the net power output can be increased by a mixture compared to the corresponding pure fluids alternatives. The optimisations furthermore suggest that the mixture composition should results in a temperature glide approximately equal to the temperature rise of the cold source. If two mixture compositions fulfil this criteria, the mixture composition should be chosen to comply with the guideline for pure fluids. That is the mixture composition should be changed from consisting of mostly the low critical temperature fluid to the higher critical temperature fluid, when the guideline of $T_{\mathrm{hf,in}} - T_{\mathrm{crit}} = [30; 50]$ K can be obtained using the higher critical temperature fluid. In that case a small amount of the lower temperature fluid should be added to make the temperature glide in the condenser match the cold source temperature rise.

5. Conclusion

In this study, the performance of an ORC system in its simplest configuration is optimised with 26 pure fluids and 3 mixtures at hot source temperatures ranging from 50 to 280°C. By optimising the ORC at different hot source temperature for a wide range of different fluid candidates with different saturation curves, generals correlations have been identified and described. By comparing the different working fluids candidates to ammonia in terms of net power output, each fluid candidate has an optimal hot source inlet temperature. By correlating this optimal hot source temperature and the critical temperature of the different fluid candidates, it is found that for a given hot source

temperature $T_{\mathrm{hf,in}}$ the optimal fluid has a critical temperature in the range [30;50] K below $T_{\mathrm{hf,in}}$. When more fluids have almost the same critical temperature such as R218 ($T_{\mathrm{crit}} = 71.9°\mathrm{C}$) and R143a ($T_{\mathrm{crit}} = 72.7°\mathrm{C}$) the fluid the the lowest ξ has a higher net work output but is more limited to the hot source temperature being [30;50] K above the critical temperature.

This optimal hot source temperature for each fluid can be explained by a better thermal match to the working fluid as the working cycles changes from sub-critical to trans-critical. The hot source temperature where the optimal cycles change from sub-critical to trans-critical will however require significantly higher heat transfer areas resulting in a lower W_{net}/A ratio. This statement is especially valid for fluids having slope of vapour saturation lines $\xi > 0$. On the other hand, fluids having $\xi \ll 0$ do not show a sudden decrease in W_{net}/A ratio.

Furthermore, working fluid suggestions are given for different hot source temperature ranges. From a hot source temperature of 50°C to 280°C, the optimal working fluids in terms of net power output are R23, ethane, R7146 (SF6), R218, R227ea, R124, R236ea, R245fa, isopentane, Pentane, R123, and R141b.

When mixtures are considered as potential working fluids, the optimal mixtures all have compositions resulting in a temperature glide approximating the cold source temperature rise. Such a temperature rise is possible by either low or high mass fractions, resulting in two possible solutions. The solution giving the required temperature glide and a critical temperature 30-50 K below the hot source temperature should be chosen. When such critical temperature cannot be obtained, the mass fraction of the mixture should be changed radically to obtain a similar temperature glide and a critical temperature.

Acknowledgement

This work is sponsored by The Danish Council for Strategic Research and the program: THERMCYC - Advanced thermodynamic cycles for low-temperature heat sources (No. 1305-00036B).

References

[1] B. F. Tchanche, G. Lambrinos, A. Frangoudakis, G. Papadakis, Low-grade heat conversion into power using organic Rankine cycles A review of various applications, Renewable and Sustainable Energy Reviews 15 (2011) 3963–3979, DOI: http://dx.doi.org/10.1016/j.rser.2011.07.024.

[2] J. Bao, L. Zhao, A review of working fluid and expander selections for organic Rankine cycle, Renewable and Sustainable Energy Reviews 24 (2013) 325–342, DOI: http://dx.doi.org/10.1016/j.rser.2013.03.040.

[3] A. I. Papadopoulos, M. Stijepovic, P. Linke, On the systematic design and selection of optimal working fluids for Organic Rankine Cycles, Applied Thermal Engineering 30 (2010) 760–769, DOI: http://dx.doi.org/10.1016/j.applthermaleng.2009.12.006.

[4] B. Saleh, G. Koglbauer, M. Wendland, J. Fischer, Working fluids for low-temperature organic Rankine cycles, Energy 32 (2007) 1210–1221, DOI: http://dx.doi.org/10.1016/j.energy.2006.07.001.

[5] E. Lemmon, M. Huber, M. McLinden, NIST Standard Reference Database 23: Reference Fluid Thermodynamic and Transport Properties-REFPROP, Version 9.1, National Institute of Standards and Technology, Standard Reference Data Program, Gaithersburg, 2013.

[6] F. Heberle, M. Preiinger, D. Grggemann, Zeotropic mixtures as working fluids in Organic Rankine Cycles for low-enthalpy geothermal resources, Renewable Energy 37 (2012) 364–370, DOI: http://dx.doi.org/10.1016/j.renene.2011.06.044.

[7] J. Radulovic, N. I. B. Castaneda, On the potential of zeotropic mixtures in supercritical ORC powered by geothermal energy source, Energy Conversion and Management 88 (2014) 365–371, DOI: http://dx.doi.org/10.1016/j.enconman.2014.08.048.

[8] Y.-R. Li, M.-T. Du, C.-M. Wu, S.-Y. Wu, C. Liu, Potential of organic Rankine cycle using zeotropic mixtures as working fluids for waste heat recovery, Energy 77 (2014) 509–519, DOI: http://dx.doi.org/10.1016/j.energy.2014.09.035.

[9] J. Andreasen, U. Larsen, T. Knudsen, L. Pierobon, F. Haglind, Selection and optimization of pure and mixed working fluids for low grade heat utilization using organic Rankine cycles, Energy 73 (2014) 204–213, DOI: http://dx.doi.org/10.1016/j.energy.2014.06.012.

[10] G. C. Prasad, c. Suresh Kumar, S. S. Murthy, G. VenKatarathnam, Performance of an organic Rankine cycle with multicomponent mixtures, Energy (2015) , DOI: http://dx.doi.org/10.1016/j.energy.2015.05.102.

[11] D. Maraver, J. Royo, V. Lemont, S. Quoilin, Systematic optimization of subcritical and transcritical organic Rankine cycles (ORCs) constrained by technical parameters in multiple, Applied Energy Applied Energy (2014) 11–29, DOI: http://dx.doi.org/10.1016/j.apenergy.2013.11.076.

[12] K. Braimakis, M. Preißinger, D. Brüggemann, S. Karellas, K. Panopoulos, Low grade waste heat recovery with subcritical and supercritical Organic Rankine Cycle based on natural refrigerants and their binary mixtures, Energy (2015) , DOI: http://dx.doi.org/10.1016/j.energy.2015.03.092.

[13] S. Lecompte, H. Huisseune, M. van den Broek, B. Vanslambrouck, M. D. Paepe, Review of organic Rankine cycle (ORC) architectures for waste heat recovery, Renewable and Sustainable Energy Reviews 47 (2015) 448–461, DOI: http://dx.doi.org/10.1016/j.rser.2015.03.089.

[14] J. Xu, C. Yu, Critical temperature criterion for selection of working fluids for subcritical pressure Organic Rankine cycles, Energy 74 (2014) 719–733, DOI: http://dx.doi.org/10.1016/j.energy.2014.07.038.

[15] C. Vetter, H.-J. Wiemer, D. Kuhn, Comparison of sub- and supercritical Organic Rankine Cycles for power generation from low-temperature/low-enthalpy geothermal wells, considering specific net power output and efficiency, Applied Thermal Engineering 51 (2013) 871–879, DOI: http://dx.doi.org/10.1016/j.applthermaleng.2012.10.042.

[16] J. Vivian, G. Manente, A. Lazzaretto, A general framework to select working fluid and configuration of ORCs for low-to-medium temperature heat sources, Applied Energy 156 (2015) 727–746, DOI: http://dx.doi.org/10.1016/j.apenergy.2015.07.005.

[17] W. Roetzel, B. Spang, C3 Typical Values of Overall Heat Transfer Coefficients, in: VDI Heat Atlas, VDI-Verlag GmbH, Düsseldorf, 75–78, iSBN: 978-3-540-77876-9, 2010.

[18] L. Cheng, D. Mewes, Review of two-phase flow and flow boiling of mixtures in small and mini channels, International Journal of Multiphase Flow 32 (2006) 183–207, DOI: http://dx.doi.org/10.1016/j.ijmultiphaseflow.2005.10.001.

[19] A. Kamei, S. W. Beyerlein, R. R. Jacobsen, Application of Nonlinear Regression in the Development of a Wide Range Formulation for HCFC-22, International Journal of Thermophysics 16 (1995) 1155–1164.

[20] S. G. Penoncello, E. W. Lemmon, R. T. Jacobsen, Z. Shan, A Fundamental Equation for Trifluoromethane (R-23), Journal of Physical and Chemical Reference Data 32 (1995) 1473–1499.
[21] R. Tillner-Roth, A. Yokozeki, An International Standard Equation of State for Difluoromethane (R-32) for Temperatures from the Triple Point at 136.34 K to 435 K and Pressures up to 70 MPa, Journal of Physical and Chemical Reference Data 26 (1997) 1273–1328.
[22] E. W. Lemmon, R. Span, Short Fundamental Equations of State for 20 Industrial Fluids, Journal of Physical and Chemical Reference Data 51 (2006) 785–850.
[23] B. A. Younglove, M. O. McLinden, An International Standard Equation of State for the Thermodynamic Properties of Refrigerant 123 (2,2-Dichloro-1,1,1-trifluoroethane), Journal of Physical and Chemical Reference Data 23 (1994) 731–779.
[24] B. de Vries, R. Tillner-Roth, H. Baehr, Thermodynamic Properties of HCFC 124, 19th International Congress of Refrigeration, The Hague, The Netherlands, International Institute of Refrigeration IVa (1995) 582–589.
[25] E. W. Lemmon, R. T. Jacobsen, A New Functional Form and New Fitting Techniques for Equations of State with Application to Pentafluoroethane (HFC-125), Journal of Physical and Chemical Reference Data 34 (2005) 69–108.
[26] R. Tillner-Roth, H. Baehr, An International Standard Formulation of the Thermodynamic Properties of 1,1,1,2-Tetrafluoroethane (HFC-134a) for Temperatures From 170 K to 455 K and Pressures up to 70 MPa, Journal of Physical and Chemical Reference Data 23 (1994) 657–729.
[27] E. W. Lemmon, R. T. Jacobsen, An International Standard Formulation for the Thermodynamic Properties of 1,1,1-Trifluoroethane (HFC-143a) for Temperatures from 161 to 450 K and Pressures to 50 MPa, Journal of Physical and Chemical Reference Data 29 (2000) 521–552.
[28] S. L. Outcalt, M. O. McLinden, A modified Benedict-Webb-Rubin equation of state for the thermodynamic properties of R152a (1,1-difluoroethane), Journal of Physical and Chemical Reference Data 25 (1996) 605–636.
[29] D. Buecker, W. Wagner, A Reference Equation of State for the Thermodynamic Properties of Ethane for Temperatures from the Melting Line to 675 K and Pressures up to 900 MPa, Journal of Physical and Chemical Reference Data 35 (2006) 205–266.
[30] M. L. Huber, J. F. Ely, A predictive extended corresponding states model for pure and mixed refrigerants including an equation of state for R134a, International Journal of Refrigeration 17 (1994) 18–31.
[31] E. W. Lemmon, M. O. McLinden, W. Wagner, Thermodynamic Properties of Propane. III. A Reference Equation of State for Temperatures from the Melting Line to 650 K and Pressures up to 1000 MPa, Journal of Chemical Engineering Data 54 (2009) 3141–3180.
[32] D. Buecker, W. Wagner, Reference Equations of State for the Thermodynamic Properties of Fluid Phase n-Butane and Isobutane, Journal of Physical and Chemical Reference Data 35 (2006) 929–1019.
[33] M. Jaeschke, P. Schley, Ideal-Gas Thermodynamic Properties for Natural-Gas Applications, International Journal of Thermophysics 16 (1995) 1381–1392.
[34] R. Tillner-Roth, H. D. Baehr, Thermodynamic Properties of Environmentally Acceptable Refrigerants: Equations of State and Tables for Ammonia, R22, R134a, R152a, and R123, Springer-Verlag Berlin, ISBN 978-3540586937, 1994.
[35] R. Span, W. Wagner, A New Equation of State for Carbon Dioxide Covering the Fluid Region from the Triple-Point Temperature to 1100 K at Pressures up to 800 MPa, Journal of Physical and Chemical Reference Data 25 (1996) 1509–1596.
[36] C. Guder, W. Wagner, A Reference Equation of State for the Thermodynamic Properties of Sulfur Hexafluoride (SF6) for Temperatures from the Melting Line to 625 K and Pressures up to 150 MPa, Journal of Physical and Chemical Reference Data 38 (2009) 33–94.
[37] B.-T. Liu, K.-H. Chien, C.-C. Wang, Effect of working fluids on organic Rankine cycle for waste heat recovery, Energy 29 (2004) 1207–1217, DOI: http://dx.doi.org/10.1016/j.energy.2004.01.004.
[38] D. Ziviani, A. Beyene, M. Venturini, Advances and challenges in ORC systems modeling for low grade thermal energy recovery, Applied Energy 121 (2014) 79–95, DOI: http://dx.doi.org/10.1016/j.apenergy.2014.01.074.
[39] W. Wagner, A. Pruss, The IAPWS Formulation 1995 for the Thermodynamic Properties of Ordinary Water Substance for General and Scientific Use, Journal of Physical and Chemical Reference Data 31 (2002) 387–535.
[40] J. H. Holland, Adaption in Natural and Artificial Systems - An Introductory Analysis with Applications to Biology, Control, and Artificial Intelligence, MIT Press, iSBN: 978-0262581110, 1992.
[41] D. Walraven, B. Laenen, W. D'haeseleer, Comparison of thermodynamic cycles for power production from low-temperature geothermal heat sources, Energy Conversion and Management 66 (2013) 220–233, DOI: http://dx.doi.org/10.1016/j.enconman.2012.10.003.
[42] Y. Dai, J. Wang, L. Gao, Parametric optimization and comparative study of organic Rankine cycle (ORC) for low grade waste heat recovery, Energy Conversion and Management 50 (2009) 576–582, DOI: http://dx.doi.org/10.1016/j.enconman.2008.10.018.
[43] M. Chys, M. van den Broek, B. Vanslambrouck, M. D. Paepe, Potential of zeotropic mixtures as working fluids in organic Rankine cycles, Energy 44 (2012) 623–632, DOI: http://dx.doi.org/10.1016/j.energy.2012.05.030.
[44] J. Fischer, Comparison of trilateral cycles and organic Rankine cycles, Energy 36 (2011) 6208–6219, DOI: http://dx.doi.org/10.1016/j.energy.2011.07.041.
[45] H. A. Ajimotokan, I. Sher, Thermodynamic performance simulation and design optimisation of trilateral-cycle engines for waste heat recovery-to-power generation, Applied Energy 154 (2015) 26–34, DOI: http://dx.doi.org/10.1016/j.apenergy.2015.04.095.

Glossary

A	Heat exchanger area, [m^2]
c_p	Specific heat capacity, [J/K kg]
h	Heat transfer coefficient, [W/m^2K]
$\dot{m}$	Mass flow rate, [kg/s]
n	Number of discretisations, [−]
P	Pressure, [Pa]
$\dot{Q}$	Heat transfer rate, [W]
R	Thermal resistance, [K/W]
s	Specific entropy, [J/K kg]
T	Temperature, [°C]
U	Overall heat transfer coefficient, [W/m^2K]
x	Quality, [−]

Greek letters

η	Efficiency, [−]
χ	Mass fraction of first-mentioned fluid, [−]
ξ	Slope of vapour saturation line, [J/K^2kg]

Subscripts

1,2,3,4	State points
cf	Cold fluid
crit	Critical state
g	Glide
hf	Hot fluid
i	index
in	Inlet
lm	Mean temperature difference
out	Outlet
pp	Pinch point
sat	Saturation state
wf	Working fluid

Nomenclature

Acronyms

ASHRAE	American Society of Heating, Refrigerating and Air-Conditioning Engineers
CAMD	Computer Aided Molecular Design
ORC	Organic Rankine Cycle
REFPROP	Reference Fluid Thermodynamic and Transport Properties Data